Synthesis and characterization of thermally stable, hydrophobic hyperbranched polyimides derived from a novel triamine

Qing Li, Haoran Xiong, Long Pang, Qiuhong Li, Ying Zhang, Wenqiu Chen, Zushun Xu and Changfeng Yi

High Performance Polymers published online 21 October 2014
DOI: 10.1177/0954008314555243

Original Article

High Performance Polymers

High Performance Polymers
1–13

DOI: 10.1177/0954008314555243
hip.sagepub.com

Synthesis and characterization of thermally stable, hydrophobic hyperbranched polyimides derived from a novel triamine

Qing Li[1,2], Haoran Xiong[2], Long Pang[1,2], Qiuhong Li[2], Ying Zhang[1,2], Wenqiu Chen[1,2,3], Zushun Xu[1,2,3] and Changfeng Yi[1,2,3]

Abstract

A novel aromatic triamide 1,3,5-tri[4-(4-aminophenoxy)phenyl] benzene (TAPOPB) with prolonged chain segments and ether bonds was successfully prepared through a three-step reaction. Then a series of hyperbranched polyimides (HBPIs) were synthesized using $A_2 + B_3$ polycondensation from various commercial aromatic dianhydrides and TAPOPB. The HBPIs showed good solubility, thermal stability with glass transition temperatures (T_g) between 218°C and 320°C, and temperature at 10% weight loss of 502.1–561.7°C in nitrogen atmosphere. Meanwhile, they had decent mechanical properties whose tensile strength and modulus were higher than 72.37 MPa and 1.039 GPa, respectively. Water uptake of less than 0.96% was obtained. The truncation wavelengths of the films were all greater than 400 nm with a good application prospect in UV protective coating. Most contact angles were more than 90°, promising to be used as hydrophobic material.

Keywords

Hyperbranched polyimide, monomer synthesis, aromatic triamide, thermal stability, surface contact angle

Introduction

Hyperbranched polymers (HBPs) have attracted widespread attention because of their unique structural characteristics and synthesis methods, and they are widely used in the fields of chemistry, physics, materials, biology, medicine, and so on.[1–5] HBPs and dendrimers constitute dendritic polymers, which show unique and distinctive properties such as low viscosity, high solubility, and a mass of terminal functional groups when compared with their linear polymers.[6,7] However, dendrimers have regular branched structures and complicated synthesis procedures. On the contrary, HBPs are prepared using an economically favorable one-step polymerization.[8–10] They are randomly branched, three-dimensional, and polydisperse macromolecules.[11,12] Moreover, they usually show similar chemical, thermal, and rheological properties to dendrimers. Therefore, HBPs are often thought to be used to replace dendrimers in many cases.[9,10] Because of the highly branched structure, HBPs are difficult to crystallize and lack a significant entanglement, resulting in a relatively good solubility. For instance, Kim et al.[13,14] reported that hyperbranched polystyrene and aromatic polyamide could be dissolved in organic solvents. However, their linear analogs were almost insoluble because of the rigidity of their backbones. Moreover, it was found that HBPs also had great potential applications in various fields such as drug delivery, molecular encapsulation, and coatings because of the hyperbranched structure and a large number of terminal functional groups.[15]

It is well known that an aromatic polyimide is an important high-performance functional material with many

[1] Ministry of Education Key Laboratory for the Green Preparation and Application of Functional Materials, Hubei University, Wuhan, China
[2] Faculty of Materials Science and Engineering, Hubei University, Wuhan, China
[3] Hubei Collaborative Innovation Center for Advanced Organic Chemical Materials, Wuhan, China

Corresponding author:
Changfeng Yi, Ministry of Education Key Laboratory for the Green Preparation and Application of Functional Materials, Faculty of Materials Science and Engineering, Hubei University, No. 368, Youyi Road, Wuchang, Wuhan 430062, China.
Email: changfengyi@hubu.edu.cn

excellent properties such as excellent thermal stability; high mechanical strength; high modulus; low coefficient of thermal expansion; and electrical, solvent resistance, and high radiation resistance properties.[16–20] As a result, they are usually applied as photoresist, separation membrane, adhesives, and matrix materials for composites.[21–26] However, their further developments and applications are often limited by their poor processability because of their limited solubility in common organic solvents, extremely high melting point, and high T_g.[27] Therefore, in this research, one aspect we focused on was the modification of polyimide, which can improve the solubility without sacrificing the outstanding comprehensive properties such as thermal properties. From the view of molecule structure design, it was reported that increasing the distance among branches and introducing flexible groups into branched units could augment physical entanglements of chains, resulting in enhanced mechanical properties and improved solubility.[28]

The cavity-containing structure of HBPIs increases the fractional free volume and makes materials display high permeability; thus, they have advantages in gas separation and are widely used as membrane materials.[29–32] Moreover, a large number of molecular terminal groups of HBPIs can be modified to create different types of multifunctional polymers.[33–35] However, studies on hydrophobicity of polyimide film are rarely reported. The studies on the hydrophobicity of the surface had drawn sustained attention. It has an extremely broad application prospect in industrial production and people's daily lives, such as snow defense, antipollution, and self-purification.[36] In general, the contact angle (CA) of the surface can reflect either hydrophilicity or hydrophobicity of the material. Hence, the aim of the present work is to also explore the surface contact angle of the HBPI film.

Usually, HBPIs are easily prepared by polymerization of AB_2 or $A_2 + B_3$ monomers in which A and B represent two different functional groups. However, AB_2 monomers are difficult to prepare because of the high reactivity between anhydride and amine groups.[37,38] Therefore, the latter method is adopted to synthesize HBPIs, and many efforts have been made toward the design and synthesis of the new triamine monomers. In this article, a novel symmetrical triamine 1,3,5-tri[4-(4-aminophenoxy)phenyl]benzene (TAPOPB) was successfully synthesized through the introduction of prolonged chain segments and ether linkages. Then, a series of HBPIs were synthesized using $A_2 + B_3$ polycondensation from various commercial aromatic dianhydrides and the prepared TAPOPB. We had synthesized a triamine 2,4,6-tris[3-(4-aminophenoxy)phenyl]pyridine (TAPP), referring to our previous work.[27] Compared with TAPP, the synthetic method of TAPOPB was more simple and convenient. Meanwhile, the HBPIs from TAPOPB possessed similar decent thermal properties, high solubility, and good mechanical properties as the HBPIs derived from TAPP. The obtained HBPIs also had potential applications in the optical and hydrophobic fields.

Experiment

Materials

Chloro-4-nitrochlorobenzene (GC, >99.5%), 4-hydroxyacetophenone (98%), silicon tetrachloride (AR), palladium on activated carbon (Pd/C, 5%), *N*-methyl-2-pyrrolidone (NMP, HPLC grade) and isoquinoline (97%) was obtained from Aladdin Reagent Inc., (Shanghai, China). Ethanol (EtOH, AR), *N*,*N*-dimethylformamide (DMF, AR), *N*,*N*-dimethylacetamide (DMAC, AR); and hydrazinehydrate (AR, 80%) were purchased from Sinopharm Chemical Reagent Co., Ltd, China. 2,2-Bis[4-(3,4-dicarboxyphenoxy)-phenyl] propane dianhydride (BPADA) and 4,4′-oxydiphthalic dianhydride (ODPA) were obtained from Shanghai Research Institute of Synthetic Resins (Shanghai, China) and 3,3′,4,4′-benzophenonetetracarboxylic dianhydride (BTDA) was purchased from Alfa Aesar, Ward Hill, Massachusetts, USA; these three kinds of tetracarboxylic dianhydrides dried in vacuo at 100°C for 12 h before use. DMF, DMAC and NMP were purified by distillation under reduced pressure over calcium hydride and were stored over 4-Å molecular sieves.

Measurements

Fourier transform infrared spectrum (FTIR) were measured using an infrared spectrophotometer (Spectrum One, Perkin-Elmer, Waltham, Massachusetts, USA), powder samples were taken into preforming with kiln-dried KBr powder. The hydrogen-1 nuclear magnetic resonance (^{1}H NMR) analysis was recorded by a Varian INOVA-400 spectrometer (Salt Lake City, Utah, USA), DMSO-d_6 as a solvent, and tetramethylsilane as an internal standard. Dynamic mechanical analysis (DMA) was performed on a TA Instruments DMA Q800 (New Castle, DE, USA) at the heating rate of 5°C min^{-1} and at the frequency of 1 Hz from 150°C to 380°C. Thermogravimetric analysis (TGA) was performed using a Perkin–Elmer TGA-7 thermogravimetric analyzer (Waltham, Massachusetts, USA) at the heating rate of 20°C min^{-1} from room temperature to 800°C under nitrogen atmosphere. Solubility was performed by putting 10 mg of polymer into 1 mL of solvent at room temperature and then observing the dissolution after 24 h. Wide-angle X-ray diffraction graphs were used to determine the crystallinity of the HBPIs by D/MAX-lllC-type X-radial diffractometer (Akishima-shi, Tokyo, Japan), taken from 5° to 80° with Cu-Kα ($\lambda = 0.154$ nm) radiation to the sample at the scanning rate of 10°C min^{-1}. The tensile properties were performed on an electronic universal testing machine (Shenzhen Sans testing machine, China) at room temperature with a pulling speed of 5 mm min^{-1}. The test films were made into samples that were 50-mm wide and 10-mm long. Water uptake (WU) was determined by immersing dried film samples into deionized water for a day at 25°C, which were then weighed after fast drying the surface moisture, and calculated as follows:

$$WU = \frac{W_s - W_d}{W_d} \times 100\%$$

Therefore, W_d and W_s were the qualities of the dried and the swollen membrane, respectively. Ultraviolet-visible (UV-Vis) spectrum of the polymer films were recorded on a Shimadzu UV-3600 instrument (Perkin-Elmer, Waltham, Massachusetts, USA). All films were controlled at a thickness of about 0.150 mm. CA test was conducted on JC2000 D instrument (Shanghai, China). Weight-average (M_w) was determined by gel permeation chromatography (GPC, Milford, Massachusetts, USA). Waters (Ultrastyragel) columns 1515 was used for GPC analysis with tetrahydrofuran (THF; 1 mL min^{-1}) as the eluent.

Synthesis of triamine monomer TAPOPB

Synthesis of 4-(4-nitrophenoxy)acetophenone (p,p-NPAP). First, 13.62 g (0.1 mol) of 4-hydroxyacetophenone, 17.28 g (0.125 mol) of anhydrous potassium carbonate, and 100 mL of dried DMAC were added into a 250-mL three-necked round-bottom flask equipped with a nitrogen inlet. The mixture was refluxed at 120°C under magnetic stirring for 3 h and then cooled to 60°C. Afterward, 15.76 g (0.1 mol) of *p*-nitrochlorobenzene was added into the mixture solution. Then, the mixture was heated up to 120°C and refluxed at this temperature for 12 h. After the reactant was cooled to room temperature, it was poured into 800 mL of EtOH/water mixture (volume ratio 1:9) to give brown precipitates and filtered and washed more than once with deionized water. Finally, 22.46 g of brown powder p,p-NPAP were obtained after recrystallization from EtOH and being dried at 60°C in a vacuum oven for 24 h.

Synthesis of 1,3,5-tris[4-(4-nitrophenoxy)phenyl]benzene (TNPOPB). Approximately 12.86 g (0.05 mol) of p,p-NPAP and 40 mL of absolute ethyl alcohol were poured into a 250-mL three-necked round-bottom flask with a dropping funnel. The top of the funnel was successively connected with a drying pipe filled with calcium chloride and an absorption apparatus for hydrogen chloride through a latex tube. Then, 14 mL (0.116 mol) of silicon tetrachloride (TCS) was added to the dropping funnel with an injector through the latex tube. TCS was added dropwise into the flask under vigorous magnetic stirring, and the mixture was continuously stirred at room temperature for 14 h after the addition was completed. At that moment, the obtained solution showed deep red, and some precipitation was generated. Subsequently, 100 mL of deionized water was poured in from the top of the condenser pipe several times. After stirring for 20 min, the mass fraction of 10% sodium hydroxide aqueous solution was added. At the moment, an orange mixture was obtained. After the product was filtrated and washed with deionized water, it was refluxed in ethyl alcohol for 30 min. A light brown powder was obtained after cooling and filtrating. Eventually, the product was recrystallized from EtOH-few CH_2Cl_2 to afford 8.25 g of buff acicular crystals.

Synthesis of 1,3,5-tris[4-(4-amidophenoxy)phenyl]benzene (TAPOPB). To a 250-mL three-necked flask equipped with a reflux condenser and a dropping funnel, 7.07 g (0.01 mol) of TNPOPB, 0.6 g of palladium on activated carbon (Pd/C, 5%), and 100 mL of absolute ethyl alcohol were added. When heated to reflux temperature under magnetic stirring, 20 mL of hydrazine monohydrate was added dropwise for 2 h. Then, the mixture continued to be refluxed for 12 h and filtered while hot. Finally, the obtained filtrate was poured into 600 mL of deionized water immediately to generate white flocculent precipitate. Approximately 5.84 g of light brown powder was obtained after filtration, washed with deionized water, and dried in a vacuum oven.

Synthesis of HBPIs

Synthesis of amino-terminated HBPIs. A typical one-step procedure was applied to polycondensation of amino-terminated HBPI (AM-HBPI). First, 1.0 mmol of the TAPOPB was dissolved in 10 mL of NMP. Then the solution was poured into a 100-mL two-necked round-bottom flask and stirred under nitrogen flow. Afterward, 1.0 mmol of anhydride was also dissolved in 10 ml of NMP. The solution was subsequently added dropwise into the flask for 1 h with a dropping funnel in an ice bath. After additional magnetic stirring for half an hour, 5 drops of isoquinoline was added. Then, *m*-xylene (15 mL) was added, and the mixture was stirred for 3 h at 120°C and kept at 180°C for 24 h with a Dean–Stark trap. After cooling to room temperature, the solution was poured into EtOH. The powder precipitate was filtered off, washed thoroughly with EtOH, and finally dried at 80°C for 24 h in a vacuum oven.

Synthesis of anhydride-terminated HBPIs. Anhydride-terminated HBPIs (AD-HBPIs) were synthesized by a two-step general procedure. A solution of TAPOPB (0.5 mmol) in NMP (10 mL) was added dropwise for 1 h into the solution of dianhydride (1.0 mmol) in NMP (10 mL) in an ice bath. Then, the mixture was stirred at room temperature for 24 h to generate anhydride-terminated hyperbranched polyamic acid (HBPAA) solution. Chemical imidization was carried out by the addition of acetic anhydride (1.2 mL) and pyridine (0.6 mL). Then, the mixture was stirred at 60°C for 6 h, at 80°C for 2 h, and at 100°C for 2 h. After being cooled to room temperature, the solution was poured into EtOH. The powder precipitate was filtered off, washed thoroughly with EtOH, and finally dried at 80°C for 24 h in a vacuum oven to afford AD-HBPIs.

Membrane formation

Because AM-HBPIs were generally synthesized using a one-step method, the corresponding precursors (AM-

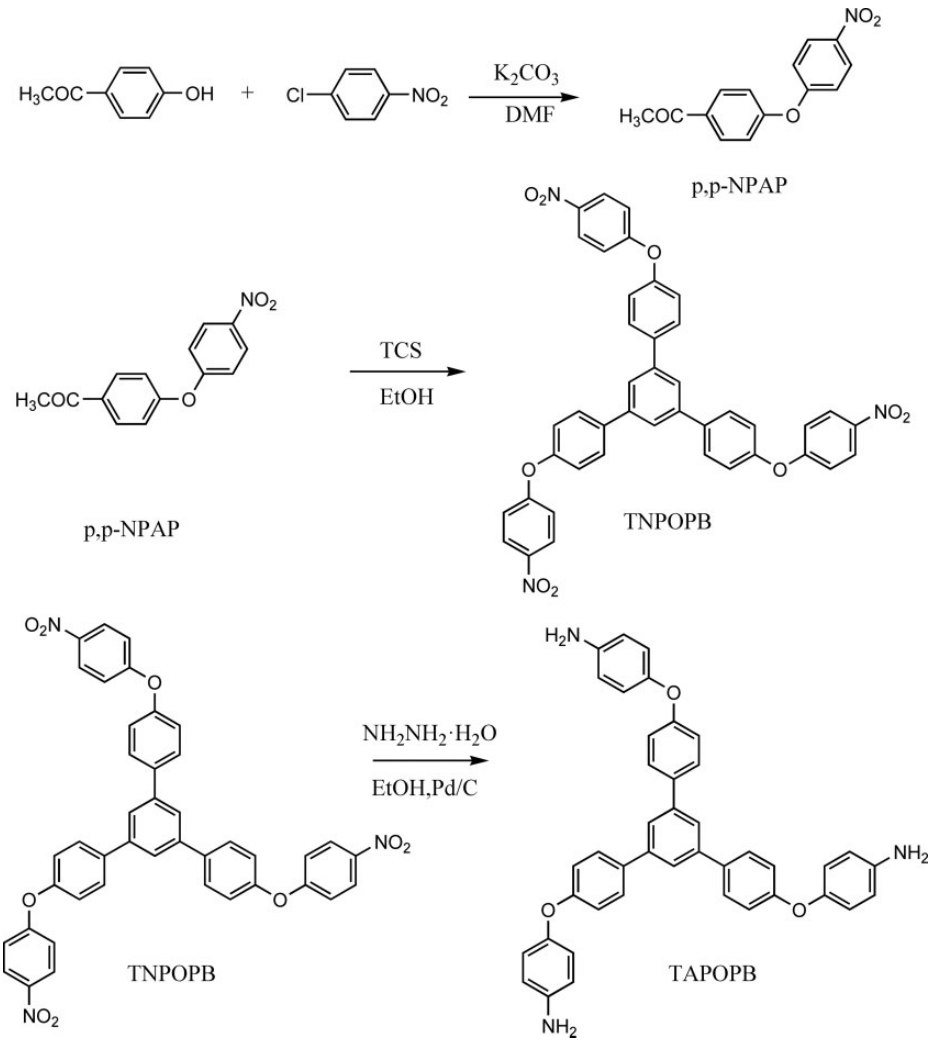

Figure 1. Synthesis of the triamine monomer TAPOPB.
TAPOPB: 1,3,5-tri[4-(4-aminophenoxy)phenyl] benzene.

HBPAAs) could not be easily obtained. Hence, we first dissolved AM-HBPI powders in a certain amount of NMP. Then, the obtained solutions were cast on dried and clean glass plates and dried at 100°C for 12 h to form the membranes of AM-HBPIs. AD-HBPI films were obtained by casting AD-HBPAA solutions on glass plates at 100°C for 12 h. Membranes were subsequently thermally imidized (150°C for 1 h, 200°C for 1 h, 250°C for 1 h, and 300°C for 1 h) in air. Finally, the membranes were determined from glass plates.

Results and discussion

Synthesis of monomer

The novel triamine monomer TAPOPB was obtained by a three-step reaction, as shown in Figure 1; 4-Hydroxyacetophenone had a nucleophilic substitution reaction with *p*-chloronitrobenzene under the effect of anhydrous potassium carbonate to produce intermediate product p,p-NPAP. Then, three molecules of p,p-NPAP had a condensation reaction in the presence of TCS/EtOH as a catalyst to give the trinitro-compound TNPOPB. TCS/EtOH is considered to be the preferred catalysts. In the synthesis of polystyrene ring macromolecules, the TCS/EtOH catalytic method was a simple and effective synthetic mean with a mild condition and a higher yield.[39] Eventually, the trinitro-compound TNPOPB was reduced to the triamine monomer TAPOPB using hydrazine hydrate as a reducing agent and Pd/C as a catalyst. The obtained triamine monomer was stable and pure at room temperature.

Infrared analysis of monomer. First, infrared spectroscopy was used to characterize the structure of the monomer, as shown in Figure 2. In the FTIR spectrum of intermediate product p,p-NPAP, the absorption peaks at about 3107 and 3072 cm^{-1} were the characteristic absorption bands of C–H in the benzene ring. The absorption peaks at about 1681 and

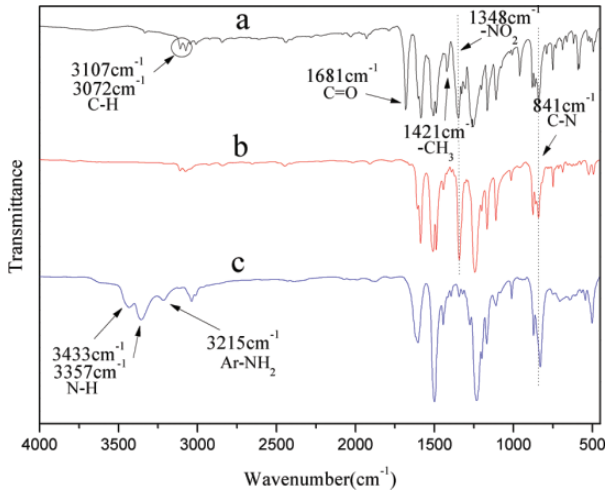

Figure 2. FTIR of (a) p,p-NPAP (b), TNPOPB, and (c) TAPOPB. FTIR: Fourier transform infrared spectrum; p,p-NPAP: 4-(4-nitrophenoxy)acetophenone; TNPOPB: 1,3,5-tris[4-(4-nitrophenoxy)phenyl]benzene; TAPOPB: 1,3,5-tri[4-(4-aminophenoxy)-phenyl] benzene.

1421 cm^{-1} were the vibration absorption peak of carbonyl C=O and the characteristic absorption peak of methyl, respectively. The absorption peaks at about 1348 and 841 cm^{-1} were the characteristic peaks of nitro group $–NO_2$ and C–N, respectively. In the FTIR spectra of trinitro-compound TNPOPB, the characteristic absorption peaks of carbonyl and methyl disappeared, whereas the characteristic absorption peaks of the nitro group still existed. It revealed that the trinitro-compound had been synthesized successfully. In the FTIR spectra of triamine monomer TAPOPB, the characteristic peaks of amino group N–H appeared at about 3433 and 3357 cm^{-1}. The vibration peak of Ar-NH_2 appeared at 3215 cm^{-1}. At the same time, the characteristic peak of the nitro group $–NO_2$ at 1348 cm^{-1} disappeared completely, proving that the nitro group was absolutely reduced to the amido group. These indicated that the target triamine monomer TAPOPB was successfully synthesized.

^{1}H NMR spectrum analysis of monomer. The ^{1}H NMR spectrum of intermediate p,p-NPAP is shown in Figure 3. As can be seen, each peak in the spectra had a very good attribution, and no miscellaneous peaks appeared. The specific attributions include ^{1}H NMR (600 MHz, DMSO-d_6, δ, ppm), 8.25 (d, $J = 7.48$ Hz, 2 H, H4), 8.03 (d, $J = 7.37$ Hz, 2 H, H1), 7.24 (d, $J = 7.22$, 2 H, H3), 7.21 (d, $J = 7.56$ Hz, 2 H, H2), and 2.55 (s, 3 H, $–CH_3$).

The ^{1}H NMR spectrum of trinitro-compound TNPOPB is shown in Figure 4. All peaks in the spectra also had good attribution, and no miscellaneous peaks appeared as well. The specific attributions are as follows: ^{1}H NMR (600 MHz, DMSO-d_6, δ, ppm), 8.26 (d, $J = 9.22$, 6 H, H1), 8.01 (d, $J = 8.62$, 6 H, H4), 7.94 (s, 3 H, H5), 7.30 (d, $J = 8.62$, 6 H, H3), and 7.18 (d, $J = 9.18$, 6 H, H2).

The ^{1}H NMR spectrum of final product triamine TAPOPB is shown in Figure 5. The new chemical shift in the peak of 4.94 was attributed to the signal peak of H proton in amido. Other peaks had corresponding attributions. It revealed that trinitro-compound TNPOPB was successfully reduced to the target triamine TAPOPB. Details are as follows: ^{1}H NMR (600 MHz, DMSO-d_6, δ, ppm), 7.72 (d, $J = 8.43$, 6 H, H4), 7.67 (s, 3 H, H5), 6.90 (d, $J = 8.46$, 6 H, H3), 6.77 (d, $J = 8.50$, 6 H, H2), 6.57 (d, $J = 8.52$, 6 H, H1), and 4.98 (s, 6 H, H6).

Synthesis of polymer

The two-step method is the most conventional synthesis method for polyimide. First, dianhydride reacted with diamine in a solvent at room temperature to give the solution of polyamic acid (PAA). Then, PAA was dehydrated to form animide ring by thermal imidization or chemical imidization to give polyimide. However, in this study, because of different order of addition and molar ratio of the obtained triamide and a variety of commercially available dianhydrides (BPADA, ODPA, and BTDA), two different end-capped HBPIs could be obtained including amino-terminated ones and anhydride-terminated ones. Amine groups could be reacted with acetic anhydride in the chemical imidization method. Thus, a one-step method was used to synthesize this class of HBPI, which made them imidized in the high boiling solvent to give products directly (dianhydride was added to triamine, and the molar ratio is 1:1). At the same time, this method could provide more energy to promote polymerization, resulting in high molecular weight (M_W) of polyimide. However, the method for AD-HBPIs was different. Triamide was first added to dianhydride to produce polyimide precursor HBPAAs at room temperature (the corresponding molar ratio is 1:2). Then, the HBPAAs were chemically converted into HBPIs with the addition of acetic anhydride and pyridine. Whether one-step or two-step method was adopted, monomer should be slowly added drop wise to avoid gelation that resulted from high concentration. Six groups of HBPI were synthesized in this experiment, as shown in Figure 6. Partial chemical structures of the HBPIs are also shown in Figure 7. D, T, and L refer to the numbers of dendritic, terminal, and linear units in the polymer, respectively. The degree of branching (DB) can characterize the structure of HBPs, generally calculated as follows:

$$\mathrm{DB} = (D + T)/(D + T + L)$$

DB had been determined from ^{1}H NMR and carbon-13 NMR spectroscopy by comparing the integration of the peaks for the respective units in the HBPs, referring to our previous work.[27] Here, we do not characterize DB anymore.

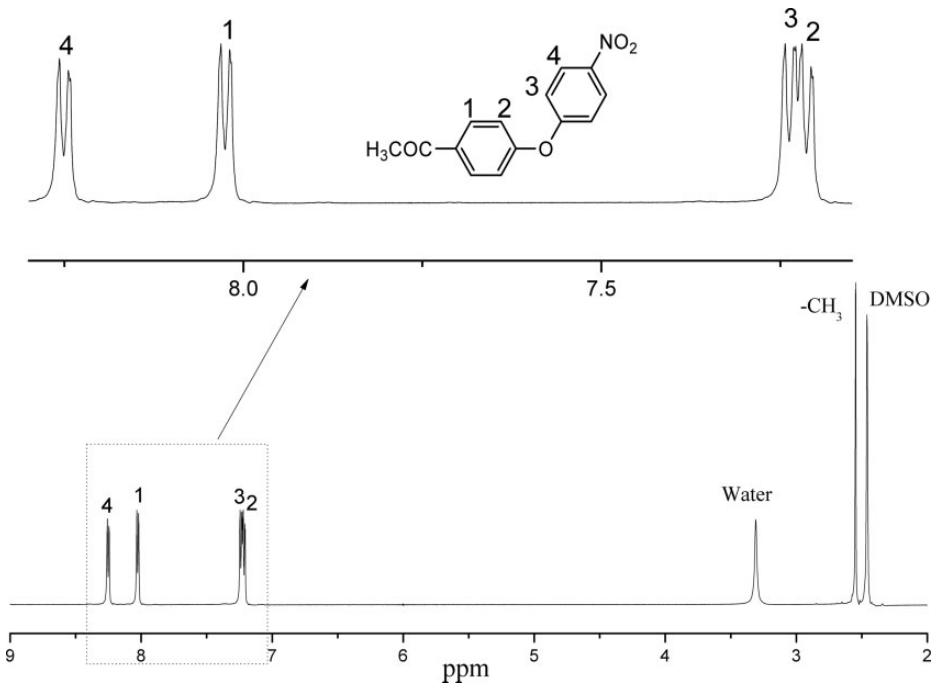

Figure 3. ^{1}H NMR spectra of p,p-NPAP.
^{1}H NMR: hydrogen-1 nuclear magnetic resonance; p,p-NPAP: 4-(4-nitrophenoxy)acetophenone.

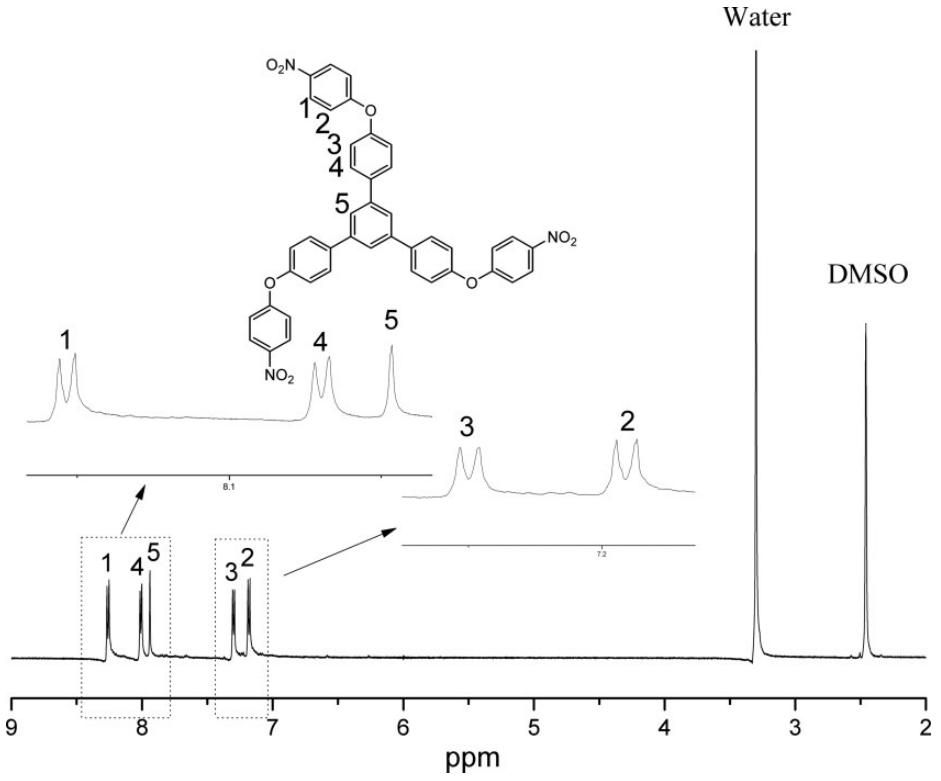

Figure 4. ^{1}H NMR spectra of TNPOPB.
^{1}H NMR: hydrogen-1 nuclear magnetic resonance; TNPOPB: 1,3,5-tris[4-(4-nitrophenoxy)phenyl]benzene.

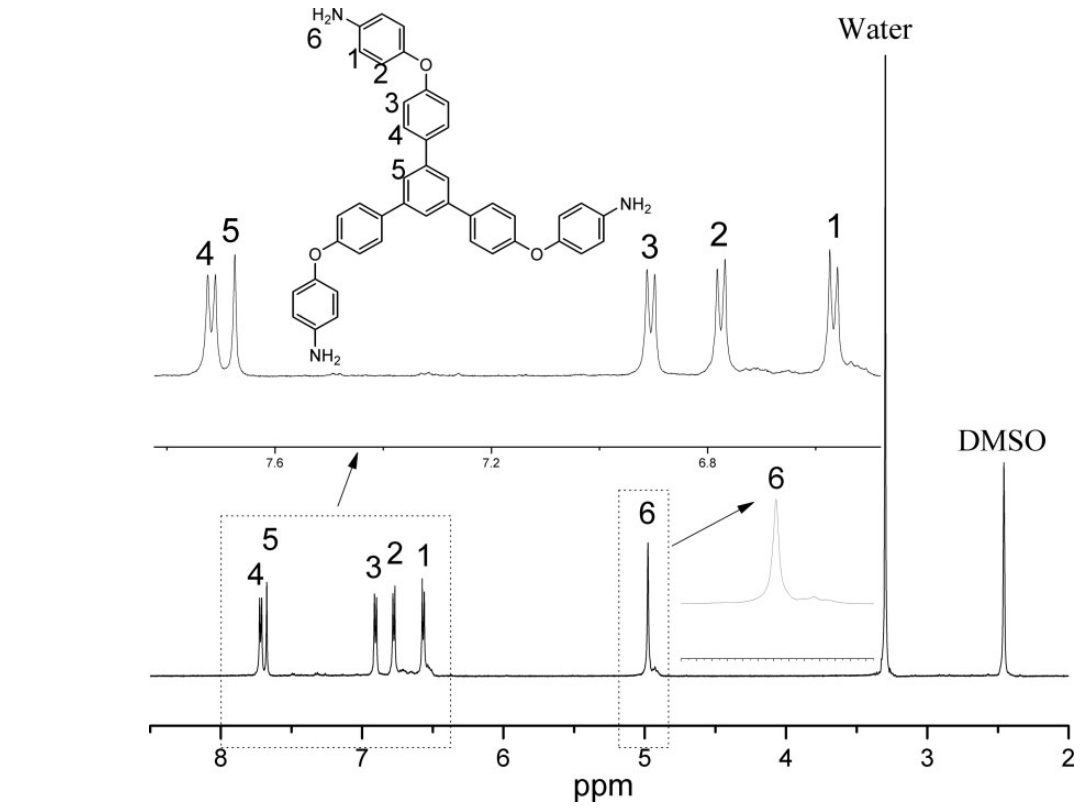

Figure 5. ^{1}H NMR spectra of TAPOPB.
^{1}H NMR: hydrogen-1 nuclear magnetic resonance; TAPOPB: 1,3,5-tri[4-(4-aminophenoxy)phenyl] benzene.

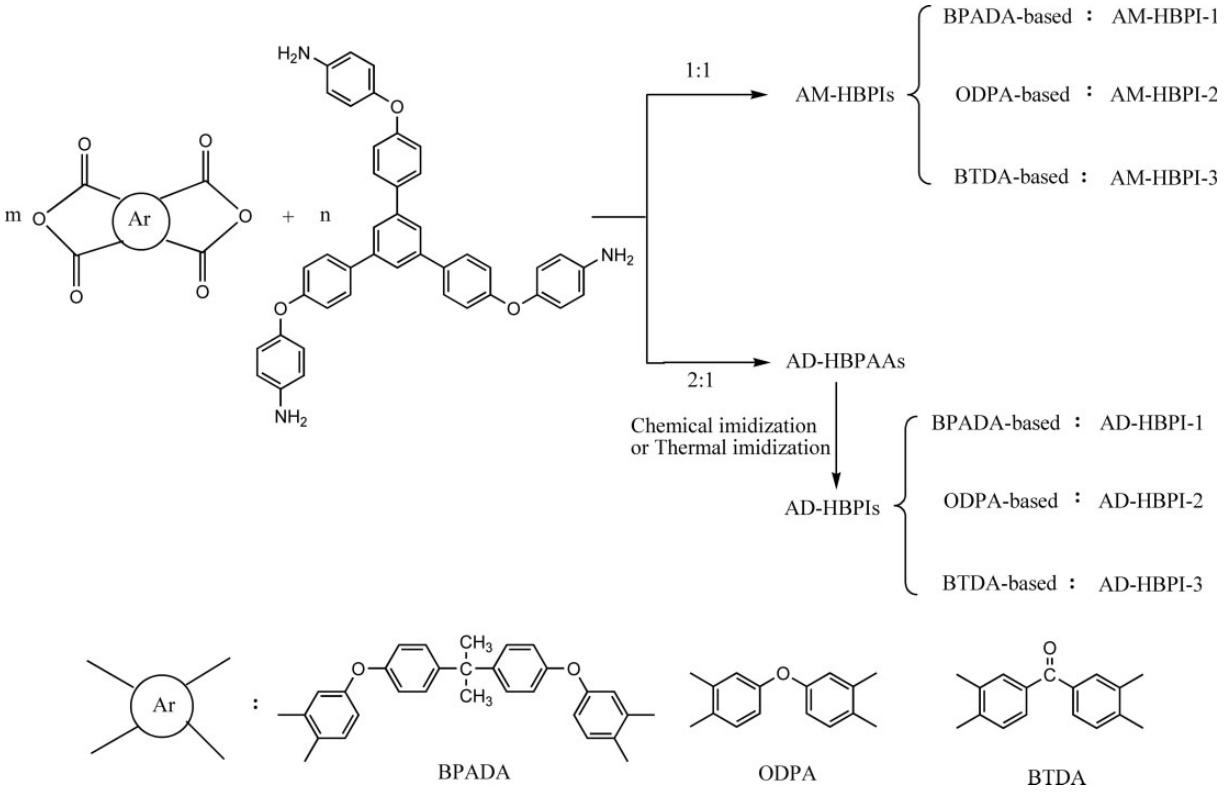

Figure 6. Synthesis of novel HBPIs.
HBPI: hyperbranched polyimide.

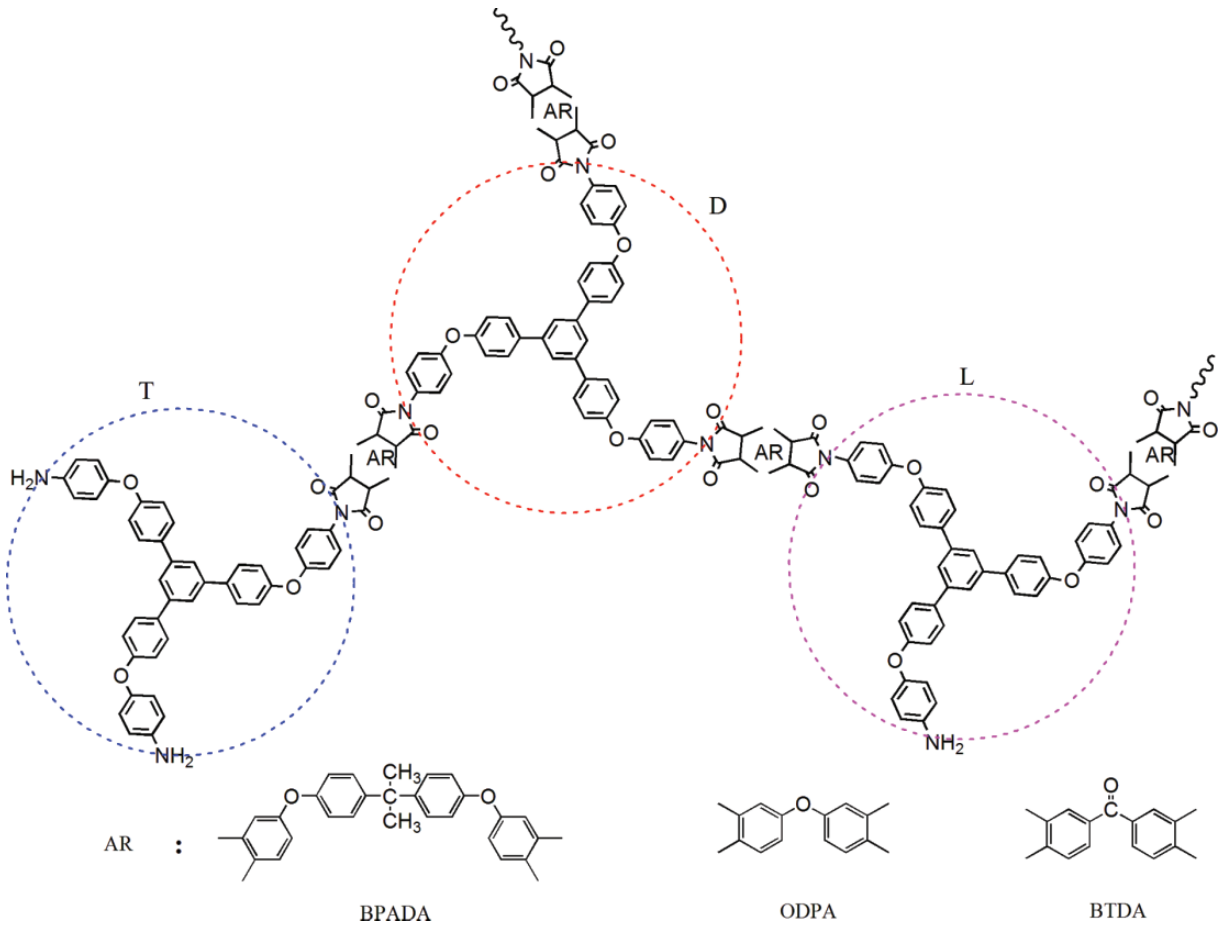

Figure 7. Partial chemical structure of the HBPIs.
HBPI: hyperbranched polyimide.

Structural characterization of HBPIs. In the infrared spectrum (IR) of HBPIs, as shown in Figure 8, the bands around 1504 and 1597 cm^{-1} are attributed to the characteristic absorption peaks of benzene ring. The bands around 1777, 1720, and 730 cm^{-1} are attributed to the asymmetric and symmetric stretching vibration peaks and bending vibration peak of the carbonyl in imide ring, respectively. The absorption band around 1376 cm^{-1} corresponds to the stretching vibration of C–N in the imide bond. In addition, the absorption peak near 1234 cm^{-1} is the absorption peak of the ether bond. The appearance of these characteristic peaks of polyimide in the IR spectra has been expected to prove the synthesis of the six HBPIs.

Morphological characterization of HBPIs. Morphological information of the HBPIs was obtained using a wide-angle X-ray diffractometer, as shown in Figure 9. In the figure, all the polyimides have blunt diffraction peaks, and there is no obvious crystallization peak. It implies that the obtained HBPIs had a low degree of crystallinity. This was mainly due to the introduction of the ether bonds, leading to

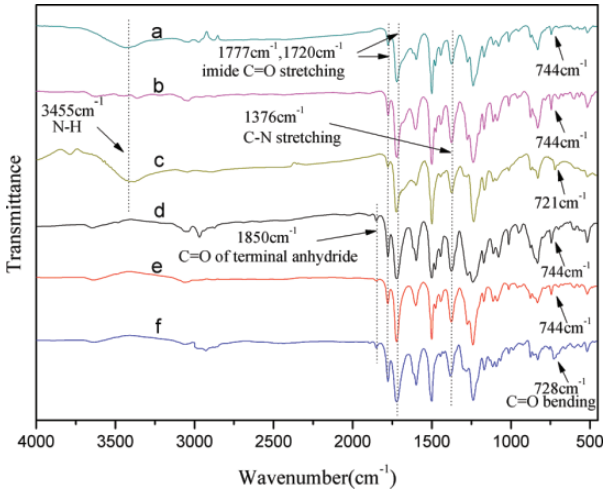

Figure 8. FTIR spectra of HBPIs: (a) AM-HBPI-1, (b) AM-HBPI-2, (c) AM-HBPI-3, (d) AD-HBPI-1, (e) AD-HBPI-2, and (f) AD-HBPI-3.
FTIR: Fourier transform infrared spectrum; HBPI: hyperbranched polyimide; AM-HBPI: amino-terminated HBPI; AD-HBPI: anhydride-terminated HBPI.

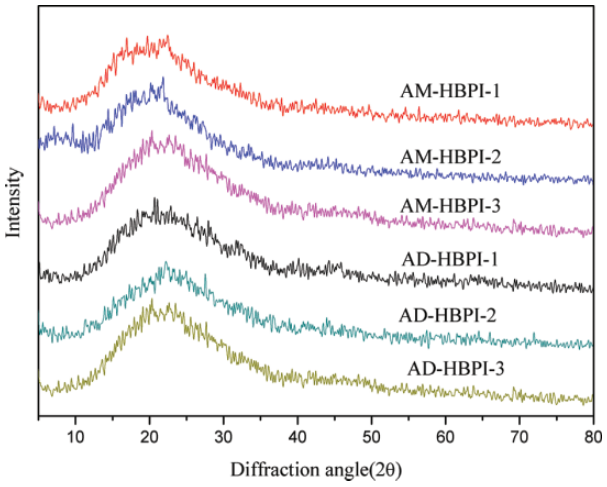

Figure 9. XRD patterns of HBPIs.
XRD: X-ray diffraction; HBPI: hyperbranched polyimide.

an increase in the flexibility of the polymer chains. Generally, a polymer with low crystallinity has good solubility, indicating that the prepared novel HBPIs should have more excellent solubility than conventional PIs.

Solubility of HBPIs. The test results for solubility of the HBPIs are shown in Table 1. The prepared HBPIs were all soluble in common polar aprotic solvents (such as DMF, DMAc, and NMP) and pyridine, except that BTDA-based HBPIs (AM-HBPI-3 and AD-HBPI-3) were partly soluble in DMF, DMAC, and pyridine. BPADA-based HBPIs were soluble in polar aprotic solvent DMSO, and ODPA- and BTDA-based HBPIs were partly soluble in DMSO. Moreover, BPADA-based HBPIs could be dissolved in protic solvents such as *m*-cresol, cyclic ethers such as THF, or chlorinated solvents such as chloroform, showing their good solubility. Solubility was also investigated when heating to 60°C, as shown in Table 1. The prepared HBPIs exhibit good solubility in organic solvents because there were three or more ether bonds and prolonged chain segments that were derived from triamide monomer in each repeating unit of the polyimide. These structures improved flexibility and increased the chain pitch to reduce the interaction between the molecular chains. Thereby, the solubility of the HBPIs was improved. Because of the absence of ether bond in BTDA, AM-HBPI-3 and AD-HBPI-3 showed poorer solubility than other corresponding HBPIs, confirming the aforementioned results.

Thermal performance of HBPIs. The thermal performance of the obtained HBPIs was investigated by TGA and DMA methods. The results are summarized in Table 2. Figure 10 shows that the storage modulus and the loss factor tan δ of the obtained HBPIs change with increasing temperature. The storage modulus decreases with increasing temperature, whereas the loss factor tan δ first increases to a peak and then declines. The temperature at the peak can be just considered as the T_g value of the polymer. It has been reported that the relative heights in T_g dispersions were inversely proportional to the volume fraction of confined segments in the interface layer. With increasing volume fraction of confined segments, the relaxation of segments at different sites in the system will span a wider temperature range.[40] The volume fraction of confined segments in the structure of BPADA, ODPA, and BTDA sequentially increased with the reduction of ether bonds. Therefore, the theory was consistent with Figure 10 ($H_1 > H_2 > H_3$, $H_4 > H_5 > H_6$), as well as the corresponding temperature range of the peak. The T_g values of the HBPIs were 270.2°C, 314.8°C, 315.5°C, 218.2°C, 255.1°C, and 291.2°C (as shown in Table 2). All of them were higher than the T_g of the commercial polyimide, Ultem 1000 (T_g, 217°C) derived from bisphenol-A diphthalic anhydride and *m*-phenylenediamine. The obtained HBPIs exhibited decent heat resistance. Under the condition of the same preparation process, the rigidity of the dianhydride monomer could affect the T_g of polyimide to some extent. In this study, BTDA, ODPA, and BPADA were in the descending order of the rigidity of dianhydride monomer. Thus, the T_gs of the corresponding polyimides gradually reduced. However, the T_gs of AM-HBPI-3 and AD-HBPI-3 were substantially higher than those of the other homologs. This was mainly because there were no flexible units such as ether linkage in dianhydride BTDA leading to the difficulty for rotation of PI chain. These could also explain why BTDA-based HBPI had slightly worse solubility.

Thermal stability of HBPIs. Because the molecules of the prepared polyimides contained a large number of imide ring and benzene ring structures, all TGA curves of the HBPIs had no significant thermal reduction below 400°C in the atmosphere of nitrogen (as shown in Figure 11). This was mainly due to the composition of the imide units that are high temperature resistant. It also illustrated that the materials were fully imidized. The decomposition temperatures at 5% (T_5) and 10% (T_{10}) weight loss were in the range of 443.8–490.3°C and 502.2–561.8°C, respectively. Moreover, the percentage of residual weights (R_w) of HBPIs at 800°C was greater than 53.8% (as shown in Table 2). These also showed that the thermal stability of the obtained polymer was good.

Mechanical properties of HBPIs. The mechanical properties of the HBPI films are shown in Table 3. It illustrated that these materials exhibited excellent film-forming and mechanical properties. Tensile strength was between 72.37 MPa and 91.01 MPa. Tensile modulus was in the range of 1.539–2.070 GPa. The toughness of the HBPI films was also good, with elongations at break from 7.36 to 13.15%. The reason why the tensile strength and elongation at break of BPADA-based HBPIs were higher than the other two

Table 1. Solubility of the prepared HBPIs.[a]

	Solvents									
	NMP	DMF	DMAC	DMSO	Py	*m*-Cresol	THF	CH_2Cl_2	$CHCl_3$	Benzene
AM-HBPI-1	++	++	++	++	++	++	++	+(++)	++	–
AM-HBPI-2	++	++	++	+(++)	++	+(+)	+(+)	–	–	–
AM-HBPI-3	++	+(++)	+(++)	+(++)	+(+)	+(+)	+(+)	–	–	–
AD-HBPI-1	++	++	++	++	++	++	++	+(++)	++	–
AD-HBPI-2	++	++	++	+(++)	++	+(+)	+(+)	–	–	–
AD-HBPI-3	++	+(+)	+(+)	+(+)	+(+)	+(+)	+(+)	–	–	–

HBPI: hyperbranched polyimide; AD-HDPI: anhydride-terminated HBPI; NMP: *N*-methyl-2-pyrrolidone; DMF: *N*,*N*-dimethyformamide; DMAC: *N*,*N*-dimethylacetamide; DMSO: dimethyl sulfoxide; Py: pyridine; THF: tetrahydrofuran.
[a]++: soluble at room temperature; +: soluble partially at room temperature; (): on heating; –: insoluble.

Table 2. Thermal properties of the HBPIs.

	Thermal properties			
Polymer	T_g (°C)	T_5 (°C)	T_{10} (°C)	R_w (%)
AM-HBPI-1	270.2	443.8	502.3	56.9
AM-HBPI-2	314.8	490.3	560.8	64.2
AM-HBPI-3	315.5	479.1	559.9	65.6
AD-HBPI-1	218.2	463.1	502.2	53.8
AD-HBPI-2	255.1	464.2	551.4	62.7
AD-HBPI-3	291.2	489.4	561.8	65.6

HBPI: hyperbranched polyimide; AM-HBPI: amino-terminated HBPI; AD-HBPI: anhydride-terminated HBPI; T_g: glass transition temperature; R_w: residual weight.

homologs was that the dianhydride monomer BPADA contained more ether bonds to make molecular chains rotate more easily. Then, the tensile strength and elongation at break were improved.

Optical properties of HBPIs. Optical property is one of the important aspects in film application. The UV-Vis spectra of PI films are illustrated in Figure 12. From the figure, we knew that all films had increased transmissivity with increasing wavelength and that the cutoff wavelengths of the obtained HBPI films were in the range of 403–531 nm, which were all higher than 400 nm. The HBPI-3 has a relatively lower optical property, reaching about 24% and 32% of transmissivity at 800 nm. These could be attributed to the increase in the intermolecular charge transfer complexes between alternating electron–donor (triamine) and electron–acceptor (dianhydride) moieties. However, the UV wavelength range of the electromagnetic spectrum was 10–400 nm which was below their cutoff wavelengths. It suggested the prepared HBPI films could absolutely absorb in whole UV, promising in the field of ultraviolet shielding coating.

Weight-average M_W*, water uptake, and surface contact angle.* According to the data from Table 4, the weight-average M_W of AM-HBPI-1 and AD-HBPI-1, which were synthesized by BPADA and TAPOPB, was 89,000 and 31,000, respectively. Because HBPs usually have a smaller size

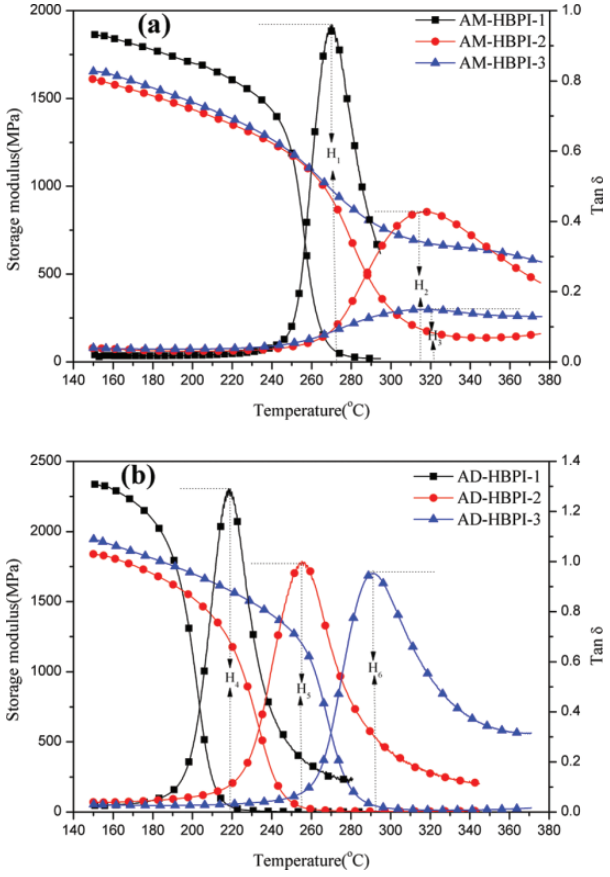

Figure 10. DMA curves of HBPIs (1 Hz, 5°C min^{-1}): (a) AM-HBPIs and (b) AD-HBPIs.
DMA: dynamic mechanical analysis; HBPI: hyperbranched polyimide; AM-HBPI: amino-terminated HBPI; AD-HBPI: anhydride-terminated HBPI.

than the linear macromolecules with the same M_W, resulting in their hard expansion to solution, the real M_W of the polymer may be larger than the measured value. The different imidization methods mainly lead to different M_Ws between AM-HBPI-1 and AD-HBPI-1. The one-step method, which was applied to AM-HBPI-1, could provide sufficient energy to the polymerization reaction and give high-M_W

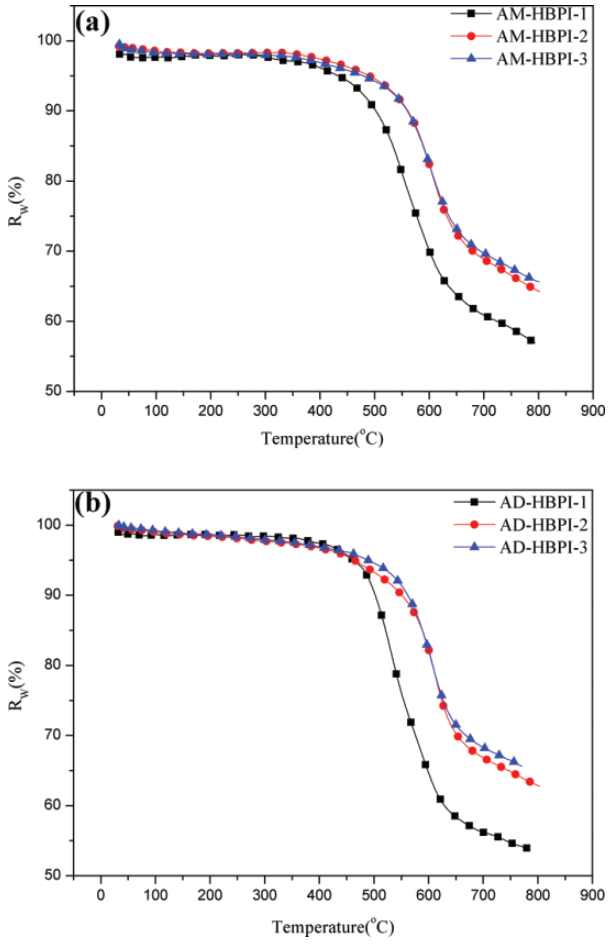

Figure 11. TG curves of the HBPIs (20°C min^{-1}): (a) AM-HBPIs and (b) AD-HBPIs.
TG: thermogravimetry; HBPI: hyperbranched polyimide; AM-HBPI: amino-terminated HBPI; AD-HBPI: anhydride-terminated HBPI.

polyimides. The M_Ws of the other polyimides could not be measured for insolubility or slight solubility in THF.

The water absorption of polyimides used in the electronics industry is an important factor, which can enhance the dielectric constant of polyimides and accelerate the corrosion of metal conductors in devices. Hence, low water uptake is extremely necessary for microelectronic manufacture. Water absorption and surface contact angle data of the HBPI films are shown in Table 4. Water absorption of the polyimide films is low, between 0.59% and 0.96%. As measurements of CA data shown in Figure 13, the CAs of all the HBPIs were more than 90° except for AM-HBPI-1, illustrating that the obtained HBPIs were basically hydrophobic. They may be promising as a kind of hydrophobic material. The result was probably attributed to the synergy of amine hydrophilic group and a large number of ether linkages in the structure of AM-HBPI-1. Thus, the surface contact angle was 76.5°, showing hydrophilic properties. However, the anhydride group is less hydrophilic than the amine group, and there are less ether linkages in the structure of HBPI-2 and HBPI-3. Therefore, the surface contact angles of AM-HBPIs were less than those of the corresponding AD-HBPIs. The combined effects also made the CA of AD-HBPI-1 greater than 90°. In general, most of the HBPIs exhibited favorable hydrophobicity, promising as a hydrophobic material.

Table 3. Mechanical properties of the HBPIs.

Polymer	Tensile strength (MPa)	Tensile modulus (GPa)	Elongation at break (%)
AM-HBPI-1	91.01	2.070	13.15
AM-HBPI-2	81.09	1.598	10.65
AM-HBPI-3	77.95	1.539	8.01
AD-HBPI-1	89.23	1.820	12.29
AD-HBPI-2	78.54	1.709	10.38
AD-HBPI-3	72.37	1.596	7.36

HBPI: hyperbranched polyimide; AM-HBPI: amino-terminated HBPI; AD-HBPI: anhydride-terminated HBPI.

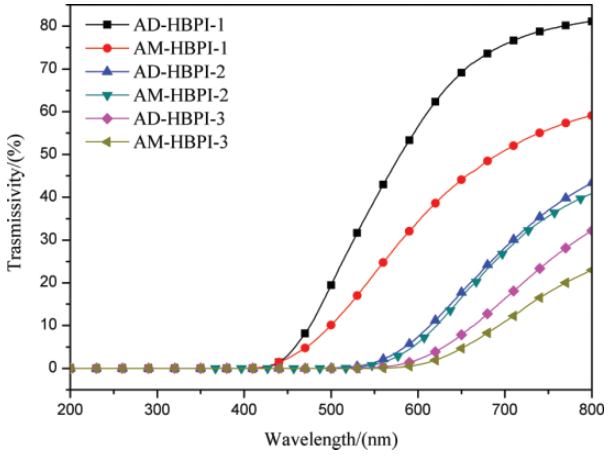

Figure 12. UV-Vis property of HBPIs.
HBPI: hyperbranched polyimide.

Table 4. Water uptake, surface contact angle, weight-average M_W, and PDI.

	M_W[a]	PDI	WU (%)	CA (°)
AM-HBPI-1	89,000	1.29	0.77	76.5
AM-HBPI-2	-[b]	-	0.60	98.7
AM-HBPI-3	-	-	0.59	99.5
AD-HBPI-1	31,000	1.58	0.83	92.0
AD-HBPI-2	-	-	0.96	100.3
AD-HBPI-3	-	-	0.80	102.5

M_W: molecular weight; PDI: polydispersity index; HBPI: hyperbranched polyimide; AM-HBPI: amino-terminated HBPI; AD-HBPI: anhydride-terminated HBPI; GPC: gel permeation chromatography; THF: tetrahydrofuran.
[a] The weight-average M_w and PDI were measured by GPC using THF solution.
[b] Not measured for insoluble or slightly soluble in THF.

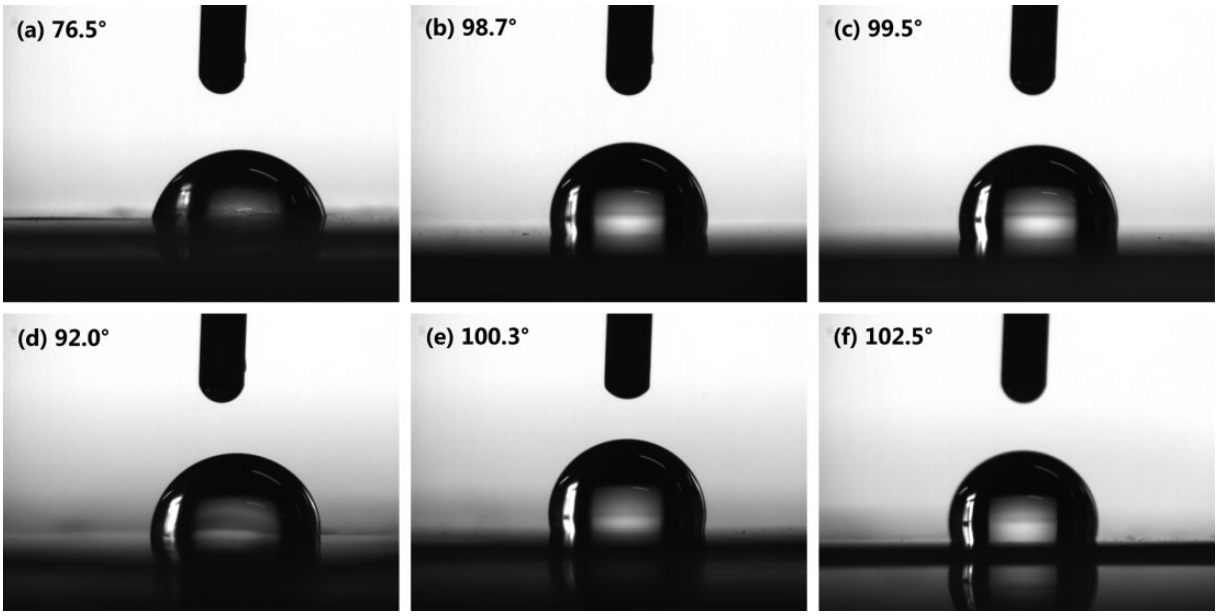

Figure 13. Surface contact angle of HBPIs: (a) AM-HBPI-1, (b) AM-HBPI-2, (c) AM-HBPI-3, (d) AD-HBPI-1, (e) AD-HBPI-2, and (f) AD-HBPI-3. HBPI: hyperbranched polyimide; AM-HBPI: amino-terminated HBPI; AD-HBPI: anhydride-terminated HBPI.

Conclusions

A novel aromatic triamide TAPOPB with three symmetrical prolonged chain segments and ether bonds was successfully synthesized. Then, a series of AM- and AD-HBPIs were successfully prepared derived from the obtained triamide TAPOPB and commercial aromatic dianhydrides (BPADA, ODPA, and BTDA). We proved that the triamine monomer and HBPIs were prepared as expected and made pure and stable by FTIR and ^{1}H NMR. The obtained HBPIs had a low degree of crystallinity and amorphous morphology, showing good solubility in many common polar aprotic solvents. Meanwhile, the HBPIs also exhibited good heat resistance, thermal stability, and mechanical properties. With good UV absorption, the polyimide films might be promising in the field of ultraviolet shielding coating. They also had low water absorption, and most of them exhibited hydrophobic property. Therefore, more in-depth research can be conducted on these particular properties.

Acknowledgement

The research was financially supported by the Natural Science Foundation of Hubei Province (2013CFB007), Hubei, China. Authors also acknowledge the Ministry-of-Education Key Laboratory for the Green Preparation and Application of Functional Materials for providing necessary facilities.

References

1. Zhang AF, Shu LJ, Bo ZS, et al. Dendronized polymers: recent progress in synthesis. *Macromol Chem Phys* 2003; **204**: 328–339.
2. Voita B. The potential of cycloaddition reactions in the synthesis of dendritic polymers. *New J Chem* 2007; **31**: 1139–1151.
3. Hobzova R, Peter J and Sysel P. Hypervetvene polymery. *Chem Listy* 2008; **102**: 906–913.
4. Voit BI and Lederer A. Hyperbranched and highly branched polymer architectures –synthetic strategies and major characterization aspects. *Chem Rev* 2009; **109**: 5924–5973.
5. Kozlowska MK, Jurgens BF, Schacht CS, et al. Phase behavior of hyperbranched polymer systems: experiments and application of the perturbed-chain polar SAFT equation of state. *J Phys Chem B* 2009; **113**: 1022–1129.
6. Hirao A, Watanabe T, Ishizu K, et al. Precise synthesis and characterization of fourth-generation dendrimer-like star-branched poly(methyl methacrylate)s and block copolymers by iterative methodology based on living anionic polymerization. *Macromolecules* 2009; **42**: 682–693.
7. Chen H and Yin J. Synthesis and characterization of hyperbranched polyimides with good organosolubility and thermal properties based on a new triamine and conventional dianhydrides. *J Polym Sci Polym Chem* 2002; **40**: 3804–3814.
8. Cabanetos C, Blart E, Pellegrin Y, et al. Synthesis and second-order nonlinear optical properties of a crosslinkable functionalized hyperbranched polymer. *Eur Polym J* 2012; **48**: 116–126.
9. Yamanaka K, Jikei M and Kakimoto M. Preparation of hyperbranched aromatic polyimide without linear units by end-capping reaction. *Macromolecules* 2001; **34**: 3910–3915.
10. Fang JH, Kita H and Okamoto K. Hyperbranched polyimides for gas separation applications. 1. synthesis and characterization. *Macromolecules* 2000; **33**: 4639–4646.

11. Voit B. New developments in hyperbranched polymers. *J Polym Sci Polym Chem* 2000; **38**: 2505–2525.
12. Inoue K. Functional dendrimers, hyperbranched and star polymers. *Prog Polym Sci* 2000; **25**: 453–471.
13. Kim YH and Webster OW. Hyperbranched polyphenylenes. *Macromolecules* 1992; **25**: 5561–5572.
14. Kim YH. Lyotropic liquid crystalline hyperbranched aromatic polyamides. *J Am Chem Soc* 1992; **114**: 4947–4948.
15. Wang L, Jin SL and Wang NX. One-step self-assembly fabrication of amphiphilic hyperbranched polymer composite membrane from aqueous emulsion for dye desalination. *J Membrane Sci* 2014; **452**: 143–151.
16. Zhao L, Yao HY and Liu Y. Synthesis and properties of novel hyperbranched polyimides end-capped with metallophthalocyanines. *J Appl Polym Sci* 2013; **128**: 3405–3410.
17. Seyedjamali H and Pirisedigh A. Synthesis and morphology of new functional polyimide/titania nano hybrid materials. *J Mater Sci* 2011; **46**: 6744–6750.
18. Hu BL, Wei HB, Han Y, et al. Low dielectric constant and organosolubility of polyimides derived from unsymmetric phthalic-thioether-naphthalic dianhydrides. *J Mater Sci* 2011; **46**: 1512–1522.
19. Chung CL, Lee WF, Lin Ch, et al. Highly soluble fluorinated polyimides based on an asymmetric bis(ether amine): 1,7-bis(4-amino-2-trifluoromethylphe noxy)naphthalene. *J Polym Sci Pol Chem* 2009; **47**: 1756–1770.
20. Düsselberg D, Verreault D, Koelsch P, et al. Synthesis and characterization of novel, soluble sulfur-containing copolyimides with high refractive indices. *J Mater Sci* 2011; **46**: 4872–4879.
21. Xiao YC, Low BT, Hosseini SS, et al. The strategies of molecular architecture and modification of polyimide-based membranes for CO_2 removal from natural gas: a review. *Prog Polym Sci* 2009; **34**: 561–580.
22. Song ZP, Zhan H and Zhou YH. Polyimides: promising energy-storage materials. *Angew Chem* 2010; **49**: 8444–8448.
23. Zhang AQ, Li XD, Nah CW, et al. Facile modifications of a polyimide via chloromethylation.I. novel synthesis of a new photosensitive polyimide. *J Polym Sci Polym Chem* 2003; **41**: 22–29.
24. Negi YS, Damkale SR and Ansari S. Photosensitive polyimides. *J Macromol Sci Polym Rev* 2001; **41**: 119–138.
25. Chen CJ, Yen HJ, Chen WC, et al. Novel high-performance polymer memory devices containing $(OMe)_2$ tetraphenyl-p-phenylenediamine moieties. *J Polym Sci Polym Chem* 2011; **49**: 3709–3718.
26. Ye YS, Huang YJ, Cheng CC, et al. A new supramolecular sulfonated polyimide for use in proton exchange membranes for fuel cells. *Chem Commun* 2010; **46**: 7554–7556.
27. Shen J, Zhang Y, Chen WQ, et al. Synthesis and properties of hyperbranched polyimides derived from novel triamine with prolonged chain segments. *J Polym Sci Polym Chem* 2013; **51**: 2425–2437.
28. Peter J, Khalyavina A, Kríz J, et al. Synthesis and gas transport properties of ODPA–TAP–ODA hyperbranched polyimides with various comonomer ratios. *Euro Polym J* 2009; **45**: 1716–1727.
29. Sim YH, Wang H, Li FY, et al. High performance carbon molecular sieve membranes derived from hyperbranched polyimide precursors for improved gas separation applications. *Carbon* 2013; **53**: 101–111.
30. Suzuki T and Yamada Y. Effect of thermal treatment on gas transport properties of hyperbranched polyimide–silica hybrid membranes. *J Membrane Sci* 2012; **417–418**: 193–200.
31. Peter J, Kosmala B and Bleha M. Synthesis of hyperbranched copolyimides and their application as selective layers in composite membranes. *Desalination* 2009; **245**: 516–526.
32. Suzuki T, Miki M and Yamada Y. Gas transport properties of hyperbranched polyimide/hydroxy polyimide blend membranes. *Eur Polym J* 2012; **48**: 1504–1512.
33. Cao ZJ, Jin L, Liu Y, et al. Crosslinkable fluorinated hyperbranched polyimide for thermo-optic switches with high thermal stability. *J Appl Polym Sci* 2013; **12**: 7607–7611.
34. Ruggerone R, Geiser V, Vacche SD, et al. Immobilized polymer fraction in hyperbranched polymer/silica nanocomposite suspensions. *Macromolecules* 2010; **43**: 10490–10497.
35. Xiao YC, Chung TS and Chng ML. Surface characterization, modification chemistry, and separation performance of polyimide and polyamidoamine dendrimer composite films. *Langmuir* 2004; **20**: 8230–8238.
36. Guo ZG and Liu WM. Progress in biomimicing of superhydrophobic surface. *Prog Chem* 2006; **18**: 721–726.
37. Chen Y, Zhang QY, Sun WL, et al. Synthesis, characterization and properties of TAP-6FDA hyperbranched polyimides with different branching degrees. *Polym Int* 2014; **63**: 788–795.
38. Hao JJ, Jikei M and Kakimoto M. Preparation of hyperbranched aromatic polyimides via $A_2 + B_3$ approach. *Macromolecules* 2002; **35**: 5372–5381.
39. Elmersy SS, Pelter A and Smith K. The direct production of tri- and hexa-substituted benzenes from ketones under mild conditions. *Tetrahedron Lett* 1991; **32**: 4175–4176.
40. Pan YZ, Xu Y, An L, et al. Hybrid network structure and mechanical properties of rodlike silicate/cyanate ester nanocomposites. *Macromolecules* 2008; **41**: 9245–9258.